Supporting Information

Zeolite-Templated Carbon as an Ordered Microporous Electrode for Aluminum Batteries

Nicholas P. Stadie[#], Shutao Wang[#], Kostiantyn Kravchyk, and Maksym V. Kovalenko*

Laboratory of Inorganic Chemistry, ETH Zürich, Vladimir Prelog Weg 1, CH-8093 Zürich, Switzerland

Empa - Swiss Federal Laboratories for Materials Science & Technology, Überlandstrasse 129, CH-8600 Dübendorf, Switzerland

[#] These authors contributed equally to this work.

* Email: mvkovalenko@ethz.ch

Synthesis of ZTC

The synthesis of fully replicate zeolite-templated carbon (ZTC) has been reviewed elsewhere[1]; the work herein benefits specifically from the use of the two-step[2-3] (liquid then vapor phase) impregnation method, and control is further improved by the use of a low-pressure CVD reactor design.

The zeolite template (HSZ 320NAA, Tosoh Corp.) was degassed at 300 °C for 24 h under vacuum (10^{-3} mbar) and 2 g of dried zeolite were combined with 10 mL of furfuryl alcohol (FA, 99%, Aldrich) under dry argon atmosphere. This mixture was stirred at room temperature for 24 h, and the solid was then collected by vacuum filtration in air. The solid was washed 3 times with 10 mL aliquots of mesitylene (97%, Aldrich) and dried on the filter frit for 15 min. The FA-impregnated zeolite was then placed in an alumina boat (10×30×107 mm) which was inserted into a custom quartz tube (ø 35 mm) and installed in a horizontal tube furnace (FST 13/70/500, Carbolite Gero). The tube was evacuated and refilled with dry argon up to 1 mbar and held under flow at 200 sccm. The FA was first polymerized by heating up to 150 °C via a 2 h ramp and held for 12 h. The poly-FA was then carbonized by heating up to 700 °C via a 2 h ramp and held for 1 h. To perform propylene CVD at 700 °C, the gas flow was then switched to 7 mol% propylene in nitrogen (99.999%, Messer Schweiz AG) at 200 sccm and the outflow was throttled to achieve a constant pressure of 250±5 mbar in the deposition zone. After 3 h, the flow was switched back to dry argon at 200 sccm and the system pressure was returned to 1 mbar. The zeolite-carbon composite was annealed by heating up to 900 °C via a 1 h ramp and held for 3 h. Finally, the system was cooled overnight, the gas flow was stopped, and the zeolite-carbon composite was removed and dissolved in 45 mL of aqueous hydrofluoric acid (HF, 40%, Sigma-Aldrich) in air. The HF was replaced 1-2 times until the siliceous material was completely dissolved (as determined by the residual mass of the solid combustion product at 1000 °C). The ZTC was collected by centrifugation, washed 5 times with 50 mL aliquots of water, and dried in air at 80 °C. Before electrode preparation and characterization, the ZTC was further dried/degassed at 200 °C under rough vacuum (10^{-3} mbar) for 12 h.

Synthesis of Ordered Porous Carbons ZDC25, MTC21, and MTC31

Additional ordered porous carbon materials were prepared similarly to ZTC for comparison purposes. A zeolite-derived carbon (ZDC25) was prepared identically to ZTC except with a lower pressure of the propylene/N_2 mixture during CVD: 200±5 mbar. The surface area was slightly reduced while the pore-to-pore ordering was drastically reduced, as indicated by N_2 adsorption measurements and X-ray diffraction, respectively. Two mesoporous templated carbons (MTC21 and MTC31) were also prepared identically to ZTC except that the template used was an ordered mesoporous silica: SBA-15 (777242, Aldrich) and MSU-H (643637, Aldrich), respectively. The surface area and pore size were found to be similar to materials reported elsewhere.[4] A commercial sample of ordered mesoporous carbon CMK-3 (ACS Material, LLC) was also investigated.

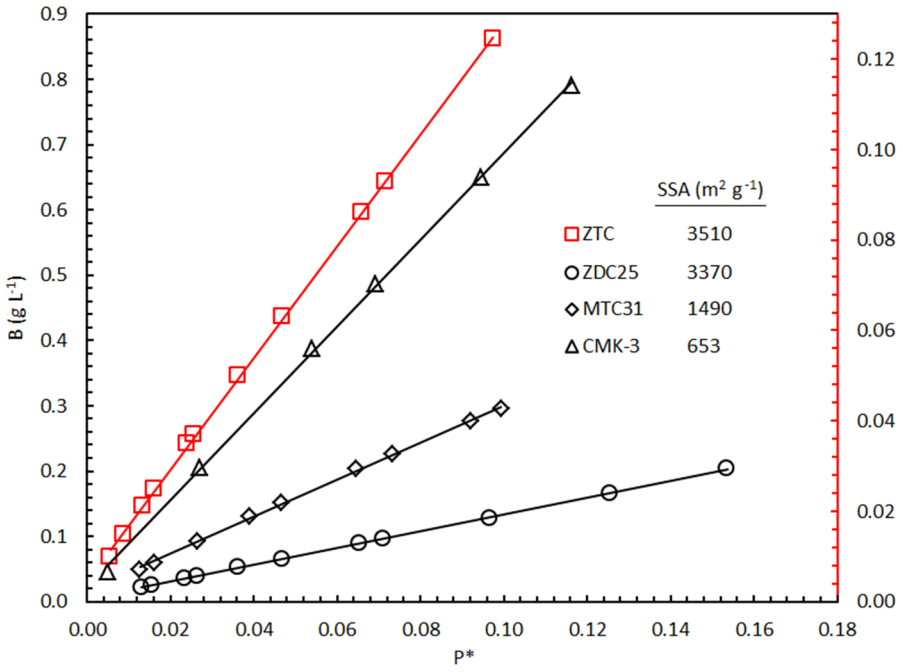

Figure S1. Brunauer-Emmett-Teller (BET) plot of N_2 adsorption uptake on ZTC at 77 K for comparison to ZDC25, MTC31, and commercially obtained CMK-3., where P* = P/P_0 and the BET variable is $B = P^*/(1-P^*)/(v_{STP})$. The calculated BET surface areas are also shown.

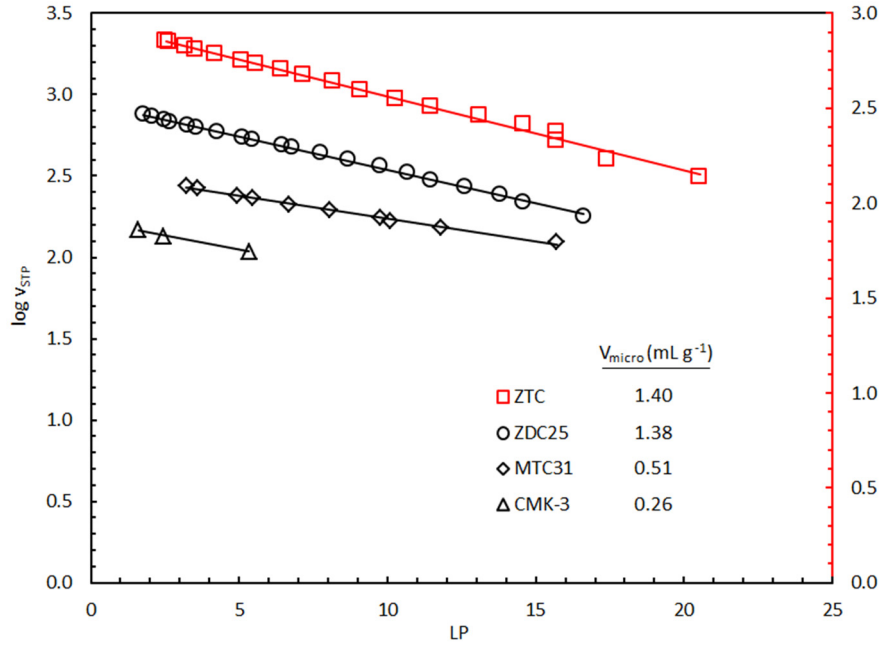

Figure S2. Dubinin-Radushkevich (DR) plot of N_2 adsorption on ZTC at 77 K, for comparison to ZDC25, MTC31, and commercially obtained CMK-3, where LP = $(\log (1/P^*))^2$. The calculated DR micropore volumes are also shown.

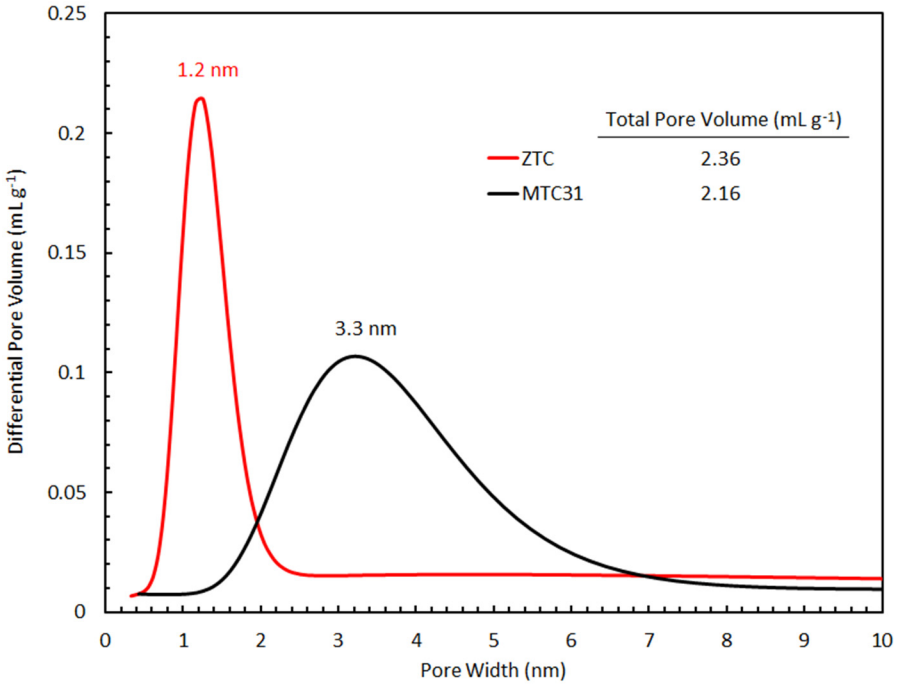

Figure S3. Non-local density functional theory (NLDFT) pore-size distribution of ZTC and MTC31, obtained based on N_2 adsorption measurements at 77 K. The corresponding total pore volumes are also shown.

Table S1. Surface and porosity properties based on N_2 adsorption at 77 K.

	BET Surface Area ($m^2\ g^{-1}$)	BET Surface Area Pressure Range (P/P_0)	DR Micropore Volume ($mL\ g^{-1}$)	NLDFT Peak Pore Size (nm)	NLDFT Total Pore Volume ($mL\ g^{-1}$)
ZTC	3510	0.005-0.10	1.40	1.2	2.36
ZDC25	3370	0.010-0.16	1.38		
MTC21	1248	0.005-0.20	0.40		
MTC31	1490	0.010-0.10	0.51	3.3	2.16
CMK-3	653	0.004-0.12	0.26		

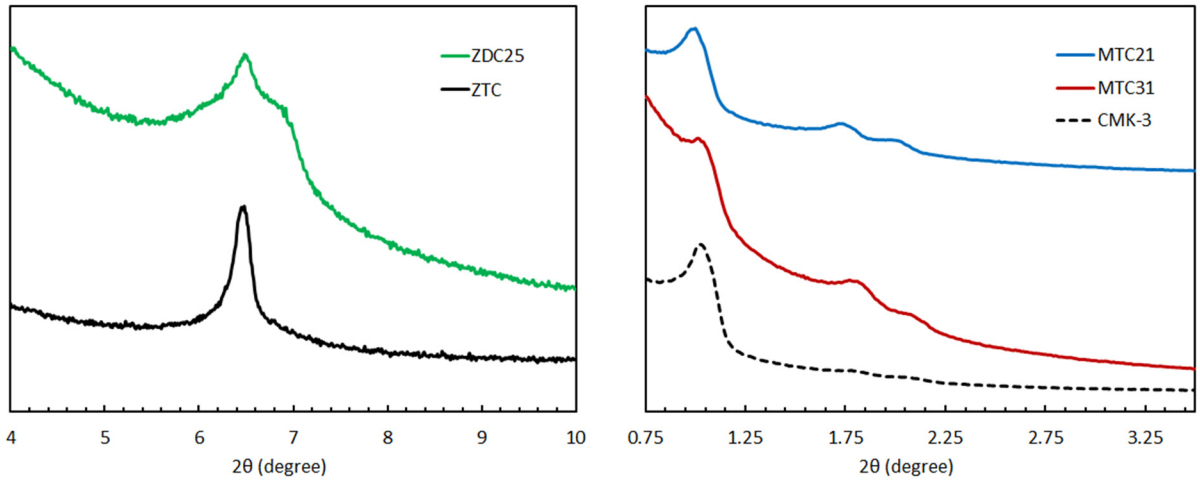

Figure S4. X-ray diffraction (XRD) patterns of the porous carbon materials shown in Table S1: ZTC, ZDC25, MTC21, MTC31, and commercial CMK-3.

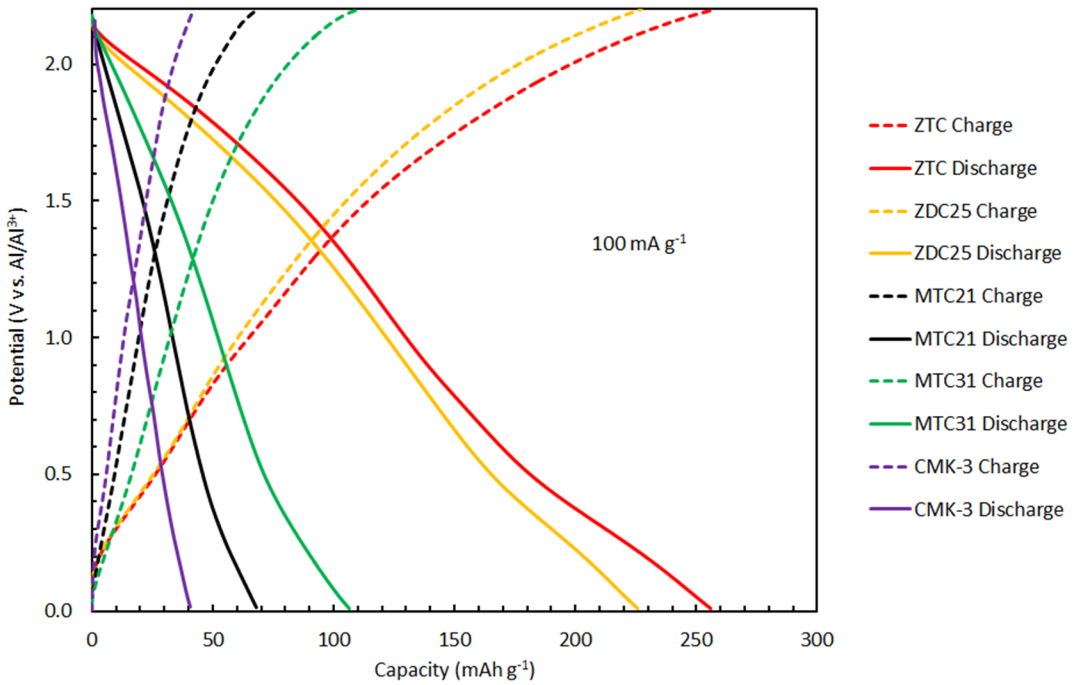

Figure S5. Galvanostatic charge/discharge voltage profiles of ZTC (red), ZDC25 (yellow), MTC21 (black), MTC31 (green), and commercial CMK-3 (purple), after 20 cycles between 0.01-2.20 V at a current rate of 100 mA g^{-1}.

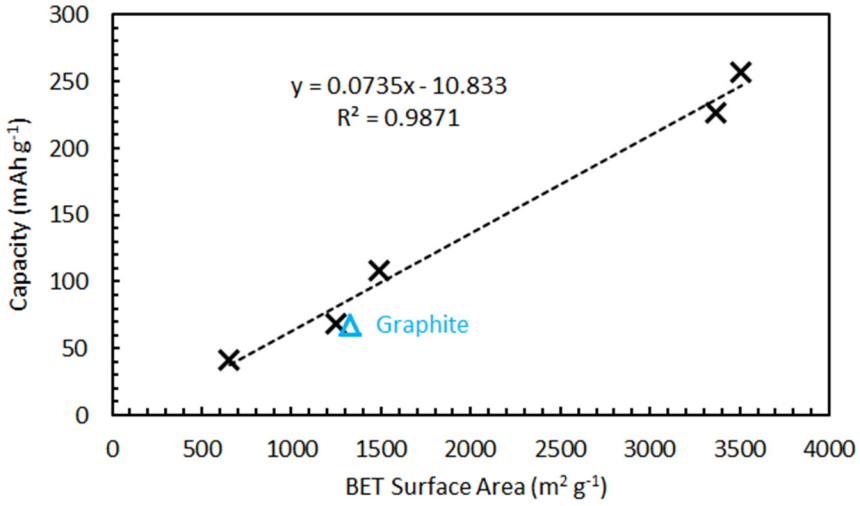

Figure S6. Reversible galvanostatic discharge capacity (between 0.01-2.20 V at 100 mA g^{-1}) as a function of BET specific surface area for the porous carbon materials shown in Table S1 (black symbols, this work), showing a linear correlation, compared to graphite (blue symbol, between 0.01-2.50 V at 66 mA g^{-1}, as reported elsewhere[5]). The "surface area" of graphite is taken to be 1311 m^2 g^{-1}, which is the real surface area of a single-sided sheet of graphene.

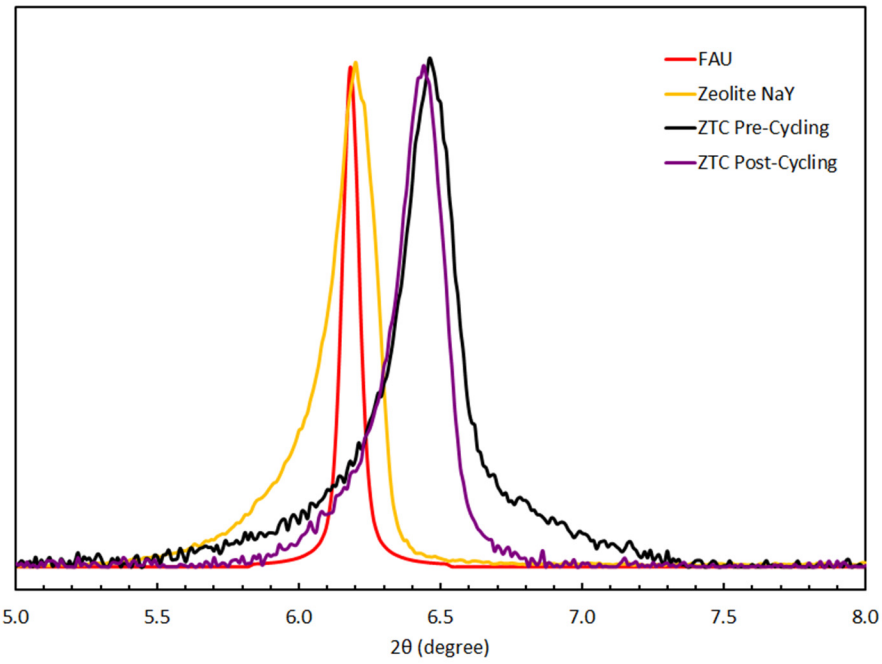

Figure S7. X-ray diffraction patterns of ZTC before and after electrochemical cycling in an AB cell (100 cycles at 100 mA g^{-1}), compared to the native template (zeolite NaY) and the theoretical faujasite framework (FAU).

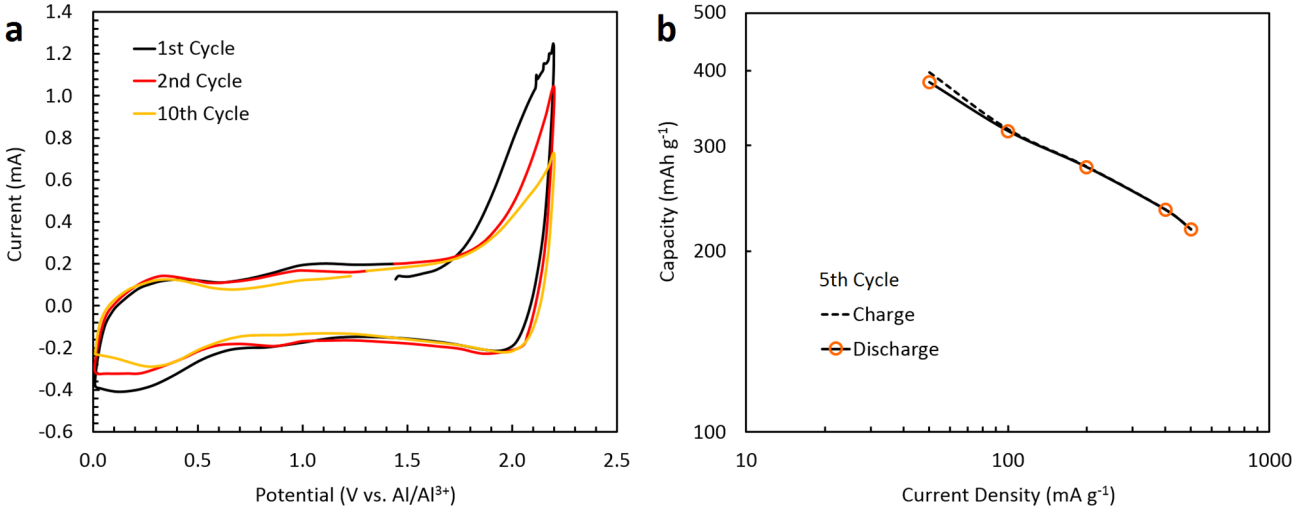

Figure S8. (a) Cyclic voltammetry measurements of a ZTC AB cell, between 0.01-2.20 V at a scan rate of 0.1 mV s^{-1}. (b) Capacity retention in the 5th cycle as a function of current rate for ZTC ABs cycled between 0.01-2.20 V.

Cathode to Cell Energy/Power Density Conversions

The precise amount of electrolyte needed for cell operation, an important factor in the determination of total cell energy density, depends significantly on which mechanism is relevant. The proposed mechanism of charge/discharge in carbon-based ABs containing the ionic liquid comprised of $AlCl_3$ in [EMIm]Cl as the electrolyte is:

$$n\ Al_2Cl_7^- + 3e^- \leftrightarrow (2n-1)\ AlCl_4^- + (4-n)\ Cl^- + Al \qquad \text{Equation S1}$$

$$\big(x(2n-1) + y(4-n)\big)\ C + (2n-1)\ AlCl_4^- + (4-n)\ Cl^- \leftrightarrow (2n-1)\ [AlCl_4]C_x + (4-n)\ [Cl]C_y + (n+3)\ e^- \qquad \text{Equation S2}$$

During the charge cycle these reactions proceed to the right, and during the discharge cycle to the left. The role of Cl^- ions in the charge storage mechanism of such ABs is not well understood (represented by "4 - *n*"). The maximum extent of intercalation of either Cl^- or $AlCl_4^-$ ions in the cathode (here represented by *x* and *y*, respectively) is left unknown.

Let us consider two extreme possibilities for the role of Cl^-: *n* = 1, where Cl^- plays a significant role, and *n* = 4, where Cl^- does not contribute to the charge storage mechanism of the AB. If Cl^- is not involved in the redox chemistry (i.e., *n* = 4), the following simple mechanism is obtained (as reported elsewhere[5]):

$$4\ Al_2Cl_7^- + 3e^- \leftrightarrow 7\ AlCl_4^- + Al \qquad \text{Equation S3}$$

$$x\ C + AlCl_4^- \leftrightarrow [AlCl_4]C_x + e^- \qquad \text{Equation S4}$$

To determine the amount of electrolyte needed to cycle the cell, we begin by finding the number of $Al_2Cl_7^-$ ions required per stored electron from the general mechanism in Equation S1 (the limiting factor to ensure electroplating of aluminum at the anode):

$$n\,Al_2Cl_7^- + 3e^- \leftrightarrow (2n-1)\,AlCl_4^- + (4-n)\,Cl^- + Al$$ Equation S1

$$mol_{Al_2Cl_7^-} = \frac{n}{3}\,mol_{e^-}$$ Equation S5

The initial $AlCl_3$:[EMIm]Cl ratio in the electrolyte (*r*) determines the amount of $Al_2Cl_7^-$ provided in the initial mixture since free Cl^- ions (from [EMIm]Cl) will combine with $AlCl_3$ to form $AlCl_4^-$ and $Al_2Cl_7^-$:

$$r\,AlCl_3 + Cl^- \rightarrow (2-r)\,AlCl_4^- + (r-1)\,Al_2Cl_7^-$$ Equation S6

$$mol_{[EMIm]Cl} = mol_{Cl^-} = \frac{1}{r-1}\;mol_{Al_2Cl_7^-}$$ Equation S7

The presence of $Al_2Cl_7^-$ is required and therefore the ratio *r* must be greater than 1 (i.e., acidic melt conditions). The practical capacity of graphite has been found to depend significantly on *r*, with a maximum at *r* = 1.3.[5] In this work, the electrolyte ratio was fixed at this optimal value across all investigations.

Together, the above equations provide the relationship between the moles of [EMIm]Cl required in the electrolyte per mole of electron stored in the cell:

$$mol_{e^-} = \frac{3}{n}\,mol_{Al_2Cl_7^-} = \frac{3}{n}\,(r-1)\,mol_{EMImCl}$$ Equation S8

$$\frac{mol_{EMImCl}}{mol_{e^-}} = \frac{n}{3}\,\frac{1}{r-1}$$ Equation S9

Since the electrolyte consists of both $AlCl_3$ (133.34 g mol^{-1}) and [EMIm]Cl (146.62 g mol^{-1}), the total mass of electrolyte (in g) per mole of [EMIm]Cl needed is then:

$$m_{electrolyte} = m_{AlCl_3} + m_{EMImCl} = 133.34\ mol_{AlCl_3} + 146.62\ mol_{EMImCl}$$ Equation S10

$$m_{electrolyte} = (133.34\ r + 146.62)\ mol_{EMImCl}$$ Equation S11

$$m_{electrolyte} = (133.34\ r + 146.62)\ \frac{n}{3}\ \frac{1}{r-1}\ mol_{e^-}$$ Equation S12

The relationship between the charge storage capacity of the cathode (*C*, in mAh g^{-1}) and the number of electrons stored, mol_{e^-}, in a fixed mass of carbon, m_C, is given by the Faraday constant, *F*, as:

$$mol_{e^-} = \frac{3.6}{F}\ C\ m_C = 3.731{\times}10^{-5}\ C\ m_C$$ Equation S13

$$m_{electrolyte} = 3.731{\times}10^{-5}\ (133.34\ r + 146.62)\ \frac{n}{3}\ \frac{1}{r-1}\ C\ m_C$$ Equation S14

*Note: *C* is used in the above equations to denote “capacity”, not the unit of “coulombs”.

Table S2. Specific capacity, energy density, and power density of a ZTC cathode and the corresponding AB cell (containing 25 mg of active material) under different mechanistic assumptions and current rates. The electrolyte composition is fixed at r = 1.3. The average cell potential at all current rates is 1.05 V.

Current Rate (mA g^{-1})	Capacity (mAh g_C^{-1})	Energy Density (Wh kg_C^{-1})	Power Density (W kg_C^{-1})	Redox Mechanism (n)	Energy Density (Wh kg_{cell}^{-1})	Power Density (W kg_{cell}^{-1})
50	382	400	52	1	64	8.3
				4	19	2.4
100	317	341	107	1	63	20
				4	19	6.0
200	276	299	216	1	61	44
				4	19	14
400	235	250	426	1	58	99
				4	18	31
500	218	230	528	1	56	129
				4	18	41
1000	159	153	960	1	46	290
				4	16	99

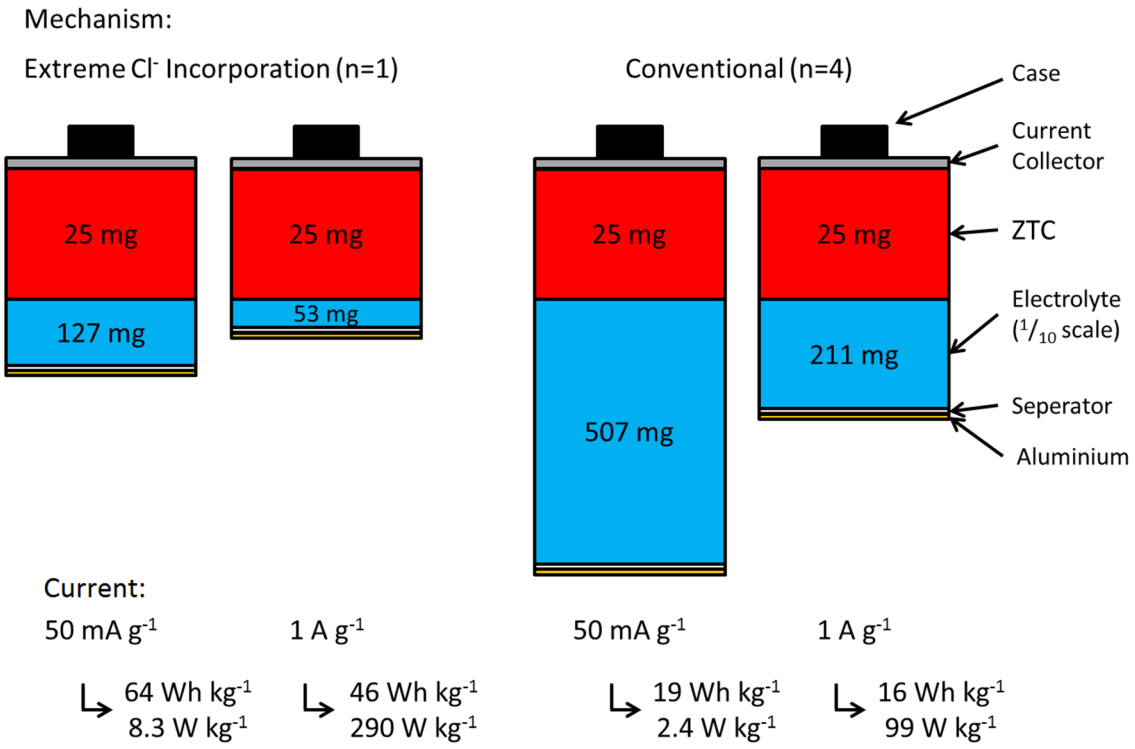

Figure S9. Mass-scaled diagrams of optimized AB cells based on ZTC as the cathode (25 mg), aluminum metal as the anode (1 mg), and $AlCl_3$ in [EMIm]Cl (r = 1.3) as the electrolyte (of variable mass). The mass of the separator (1 mg), cathodic current collector (2 mg), and case (1 mg) is also added. The amount of electrolyte required depends on the reversible capacity of the cathode (which varies as a function of current rate, see Figure 2b) and the mechanism of charge storage (from n = 1 for significant contribution from Cl^- insertion in the carbon to n = 4 for no contribution from Cl^- ions). The final, complete cell energy and power densities are shown below, which correspond to the values plotted in Figure 4 and tabulated in Table S2.

Table S3. Bulk material densities used in gravimetric to volumetric capacity calculations.

Material	Density (g mL^{-1})	Reference
ZTC	0.6	(measured)
Densified ZTC	0.9	Hou et al.[6]
Pyrolytic Graphite	2.1	(MTI Corp.)
Graphitic Foam	0.005	Chen et al.[7]

References

1. Nishihara, H.; Kyotani, T., Templated Nanocarbons for Energy Storage. *Adv. Mater.* **2012,** *24*, 4473-4498.

2. Ma, Z.; Kyotani, T.; Tomita, A., Synthesis Methods for Preparing Microporous Carbons with a Structural Regularity of Zeolite Y. *Carbon* **2002,** *40*, 2367-2374.

3. Matsuoka, K.; Yamagishi, Y.; Yamazaki, T.; Setoyama, N.; Tomita, A.; Kyotani, T., Extremely High Microporosity and Sharp Pore Size Distribution of a Large Surface Area Carbon Prepared in the Nanochannels of Zeolite Y. *Carbon* **2005,** *43*, 855-894.

4. Kim, S.-S.; Pinnavaia, T. J., A Low Cost Route to Hexagonal Mesostructured Carbon Molecular Sieves. *Chem. Commun.* **2001**, 2418-2419.

5. Lin, M.-C.; Gong, M.; Lu, B.; Wu, Y.; Wang, D.-Y.; Guan, M.; Angell, M.; Chen, C.; Yang, J.; Hwang, B.-J., et al., An Ultrafast Rechargeable Aluminium-Ion Battery. *Nature* **2015,** *520*, 324-328.

6. Hou, P.-X.; Orikasa, H.; Itoi, H.; Nishihara, H.; Kyotani, T., Densification of Ordered Microporous Carbons and Controlling Their Micropore Size by Hot-Pressing. *Carbon* **2007,** *45*, 2011-2016.

7. Chen, Z.; Ren, W.; Gao, L.; Liu, B.; Pei, S.; Cheng, H.-M., Three-Dimensional Flexible and Conductive Interconnected Graphene Networks Grown by Chemical Vapour Deposition. *Nat. Mater.* **2011,** *10*, 424-428.